

# A Novel Approach of Back-propagated Fuzzy Switching Median Filter for Medical Lung CT image denoising

**M. Jannath Firdouse**

*Research Scholar, Department of Computer Science Engineering  
Research & Development Center, Bharathiar University, Coimbatore, Tamil Nadu, India.*

**Dr. M. Balasubramanian**

*Assistant Professor, Department of Computer Science Engineering, Annamalai University, Kadallore, India.*

## Abstract

The main reason of the inefficiency of most of the image processing task is the noise occurrences on digital images. The noise distribution disturbs the image segmentation behavior and finally the result may be in deformed state which is not supported for the upcoming image processing tasks. The existing methods of denoising suffer with the non-preservation of edges and blurring. So a new method of denoising process is urgently required in order to improve the medical segmentation result. This paper proposes a novel method of denoising for medical image segmentation using the neuro- fuzzy concepts. A new method namely back propagated fuzzy switching median filter (BPFMSM) is proposed to remove the noise occurrences in medical lung images. This method works based on three divisions such as switching median filter, fuzzy based training vector generation and BPN based noise reduction. The switching median filter uses multi size windows for median filter and the fuzzy logic is initiated by maximum absolute luminance array. The back propagated based denoising is considered with training vectors and testing vector. This novel method produces great impact on medical lung segmentation because of its influence on noise suppression. The proposed BPFMSM method preserves edges while at noise suppression and the performance level of BPFMSM is better at a significant level.

**Keywords:** BPFMSM, Switching Median Filter, BPN, Fuzzy, Noise Reduction and Denoising

## INTRODUCTION

Denoising an image is an important task for correcting faults produced during the acquisition process of a realworld scene while reproducing for the display, due to physical and technological limitations [1]. It can also be appropriate as a pre-processing stage in order to improve the results of higher level applications. The problem of removing the noise of an image while preserving its main features (edges, textures, colors, contrast, etc.) has been extensively investigated over the last two decades and several types of approaches have been developed. The total variation-based denoising method of Rudin *et al.* [2] had a great impact in the imaging community and has inspired a large amount of variational formulations for image denoising. Years after the model of Rudin *et al.*, a novel

approach for image denoising based on the comparison of pixel neighborhoods such as patches was proposed simultaneously by Awate and Whitaker [3] with the UINTA algorithm and Buades *et al.* [4] with the Non-Local Means (NLM). The spatial domain and frequency domain methods are applicable for the denoising process which is depends on the specific noise. Many cases can be obtained with regard to the distribution and strength of noise in an image. For example, Tian *et al.* closely analyzed noise at the circuit level [5]. Moreover, Hirakawa and Parks proposed a novel method to remove practical noise from real-world applications.

The method described in [6] is the edge preserving capability in order to reduce the speckle noise of an ultrasound image. This utilizes the benefits of shift invariant and NSCT. This helps to capture the geometric information of the image. By applying the morphological operations with respect to the structural element and the NSCT, the directional sub bands are denoised. Median absolute deviation [7] approach is used for the denoising. This method estimates the noise variance and the signal variance with the help of the mathematical morphological operations. The drawbacks of this method are the use of high resolution images. A novel three domain fuzzy support vector regression is proposed in [8] to handle the uncertainty exist with the image. This is based on the weighted method described in [9], [10] to enhance the adaptive learning capability. 3DFSVR includes three domain fuzzy mapping function, three domain fuzzy regression hyper plane and the kernel function. The three domain fuzzy kernel function works on the fuzzy, input and output domains. The noises denoised are Gaussian noise, Salt and pepper noise and the mixed of these two noises. This method's performance is relatively high. This process can be implemented for fault diagnosis, image processing and compression and the robust identification and control.

As described in [11], a compression post processing algorithm by employing the plug and play prior's framework is involved in order to denoise the images. This is highly effective compared to K-SVD [12] and BM3D [13]. This addresses an inverse problem for a forward model that is non-linear and non-differentiable. This method is strengthened by adopting the denoiser with an oracle capability. The advanced feature implements the Gaussian denoiser with Oracle capability. The method described in [14] transforms the noisy image in to the

luma chroma color space. The texture information is transferred from the denoised luma channel to the chroma channel. If the proposed CDTT uses [13] and WNNM [15], then the improvement is made in the performance. By using the Wiener filter, the patch variance estimation can be improved.

The approach explained in [16] is based on the two way approach [17] which utilizes the RBSPP method I parallel with KRX anomaly detection prior to the extraction of end members. The extraction is on homogeneous regions instead of transition areas. These end members are used to reconstruct a denoised and destriped hyper spectral data. The performance factor is relative high compared with the other methods. The paper [18] described the computation of the components of the image to be processed in a moving frame which encodes the local geometry. This provides better results in terms of PSNR and structural similarity index. The result produced by this method is better based on the image content, noise level and the denoising method involved. Only by adding the Gaussian noise the method should be taken for the future development.

The paper [19] explains about the noise decomposition procedure which uses a local structure preserving sparse coding to display the local sparse structures. This suppresses the noise and maintains the texture. An LSPSC and Kernel LSPSC algorithm constructs the LSSD model for LLL images. The automatically and blind algorithms devoted to the complex noise Neat Image and Noise Clinic [20]. This method preserves the sparsity of patches and local structure in images. As a future work it can be extended for the non-linear algorithms. As explained in [21], the noise is reduced by applying the zero mean white Gaussian noise removal method. Two dimensional non harmonic analysis techniques are involved in this method in order to increase the noise removal accuracy. This has the feature of side lobe reduction which is explained in [22]. An edge preserving segmentation method is implemented by a compound method which consists of Canny edge detection and a mean shift algorithm. This method is inferior to other methods in terms of SSIM values.

The wavelet based denoising with a new histogram based threshold function and selection rule is proposed in [23]. The simulation results shows the merits of this method by measuring the metrics such as SNR, cross correlation coefficient, mean square error and reduction in noise level. HBTE also achieves the higher correlation coefficient and lower residual distribution. The method in [24] explains that natural stochastic textures present in the image is denoised by using patch based fractional Brownian motion model and regularization based on anisotropic diffusion. This recovers the textural and structural attributes which characterizes the natural image. Anisotropic diffusion performs the selective smoothing [25]. Advantages are its simplest autocorrelation function and the null hypothesis can be determined numerically via simulation of a large number of images.

The existing noise reduction methods are not fit for medical image segmentation. They are inconsistent with medical

application because of their blur producing habit and non-preservation of edge data. So the novel algorithm BPFMSM is attached with this research. This is an unparalleled algorithm in the denoising cases. The switching median filter, fuzzy logic and BPN are integrated to work jointly to receive the denoised medical image. The noises at heavy range can also be tested with this algorithm.

The section II explains in detail about the running method of the proposed BPFMSM noise reduction scheme. The section III shows the simulation results and discussion which provides an analysis part with the proposed method. The section IV describes the conclusion part of the research paper and section V focuses about the listing of referred papers.

## METHODS

The figure 1 explains about the working flow of the proposed method. This proposed noise reduction scheme s working based on switching median filter, fuzzy and BPN methods. The proposed BPFMSM method removes the impulse noise of any image especially medical lung images. This proposed scheme can be subdivided in to the following five sub components:

- Noisy Pixel Detection
- Switching Median Filter Computation
- Maximum Absolute Luminance Computation
- Fuzzy based BPN target array generation
- BPN based noise restoration

### a) Noisy Pixel Detection

The given medical image is read out and the pixel information are stored in the 2D array. The processing pixel is decided as noisy by checking whether the pixel is the category of the intensity value zero or 255. If the processing pixel  $P(i, j)$  belongs to the intensity value zero or 255 then that pixel is denoted as the noisy pixel and otherwise it is considered as non noisy pixel. It can be shown by the equation (1)

$$I_{NOISY} = \begin{cases} 1, & \text{if } I_{INPUT}^{i,j} = 0 \text{ || } I_{INPUT}^{i,j} = 255 \\ \text{Else } 0 & \end{cases} \quad \text{----- (1)}$$

where,  $I_{NOISY}$  = Noisy Image indicated by 1

$I_{INPUT}$  = Original Image

In the  $I_{NOISY}$  image the pixels which are own the value 1 are set as Noisy pixels and others are known as non-noisy pixels.

### b) Switching Median Filter

The switching median filter is the improved version of median filter. Here multi size windows are applied on the image and finally the suitable size of window is chosen and applied on the image to get the better noise reduced image. But this filter is

lacking of noise reduction performance by making blur data. So the new proposed method used this filter only for training purpose of neural networks and the final result is assured by BPN.

First a 3 x 3 size window is adapted to get the sum of the neighbor elements. If that sum value is not greater than zero then the window size S is incremented and applied on the medical image. Then the sum is calculated and compound with zero, and if the sum value is less than zero, the window size is increased and applied. This process is iteratively applied until the reaching of greater zero or a threshold. Finally the received window size is used to compute the switching median filter based noise reduced output. This result is a temporary result only.

**c) Maximum Absolute Luminance Calculation**

The intensity is often called as luminance. The window size ‘s’ which is the resultant of switching median filter is considered and a window which is the category of overlapped is extracted. The difference between the center element c and the neighbor element are calculated based on 3 x 3 size window. The equation used to demonstrate these are equations (2) to (10).

$$D_1 = |P(i - 1, j - 1) - c| \text{ ----- (2)}$$

$$D_2 = |P(i - 1, j) - c| \text{ ----- (3)}$$

$$D_3 = |P(i - 1, j + 1) - c| \text{ ----- (4)}$$

$$D_4 = |P(i, j - 1) - c| \text{ ----- (5)}$$

$$D_5 = |P(i, j + 1) - c| \text{ ----- (6)}$$

$$D_6 = |P(i + 1, j - 1) - c| \text{ ----- (7)}$$

$$D_7 = |P(i + 1, j) - c| \text{ ----- (8)}$$

$$D_8 = |P(i + 1, j + 1) - c| \text{ ----- (9)}$$

$$D_{MAX} = \text{Maximum } (D_1, D_2, D_3, D_4, D_5, D_6, D_7, D_8) \text{ ----- (10)}$$

where , D<sub>1</sub> to D<sub>8</sub> – absolute difference

D<sub>MAX</sub> – Maximum absolute difference

c – center pixel window of the window

The equations (2) to (10) are given for the example of processing the 3 x 3 size window. i.e. s = 3. If suppose the window size s is equal 5, then a 5 x 5 size window is used and the final maximum absolute luminance is computed for each and every pixel.

**d) Fuzzy based BPN target array generation**

The BPN needs training array and target array. The training array is prepared from the noise pixels neighbors including itself, so the vector count is 9. The target value for the BPN is

calculated using the fuzzy technique on the maximum absolute luminance difference data using the equation (11).

$$\text{Target} = \begin{cases} 0, & \text{if } \text{MALD} < T_1 \\ (\text{MALD} - T_1) / (T_2 - T_1) & \text{else if} \\ T_1 \leq \text{MALD} \ \&\& \ \text{MALD} < T_2 & \text{----- (11)} \\ 1 & \text{else} \end{cases}$$

where, Target – Target value for BPN

MALD – Maximum absolute luminance difference

T<sub>1</sub> – Threshold 1 (assume as 10)

T<sub>2</sub> – Threshold 2 (assume as 30)

**e) BPN based Noise Restoration**

The BPN network is created with the following configuration.

```
net.trainparam = 100
net.trainparam.lr = 0.92
net.trainparam.mc = 0.97
net.trainparam.epochs = 500
net.trainparam.goal = 1e - 5
```

The BPN network is trained based on the trained vectors and the corresponding target values. The noise restoration is done using the equations 12 and 13.

$$\text{Sim} = \text{Simulation} (\text{BPN\_net}, T) \text{ ----- (12)}$$

$$\text{NF} (i, j) = \begin{cases} \text{Sim} * p^{i,j}, & \text{if } \text{Sim} < 0 \\ (1 - \text{Sim}) * p^{i,j}, & \text{else if} \\ \text{Sim} \leq 0.8 & \text{----- (13)} \\ \text{SMF else} \end{cases}$$

where, Sim - testing of BPN result

Simulation – simulation function

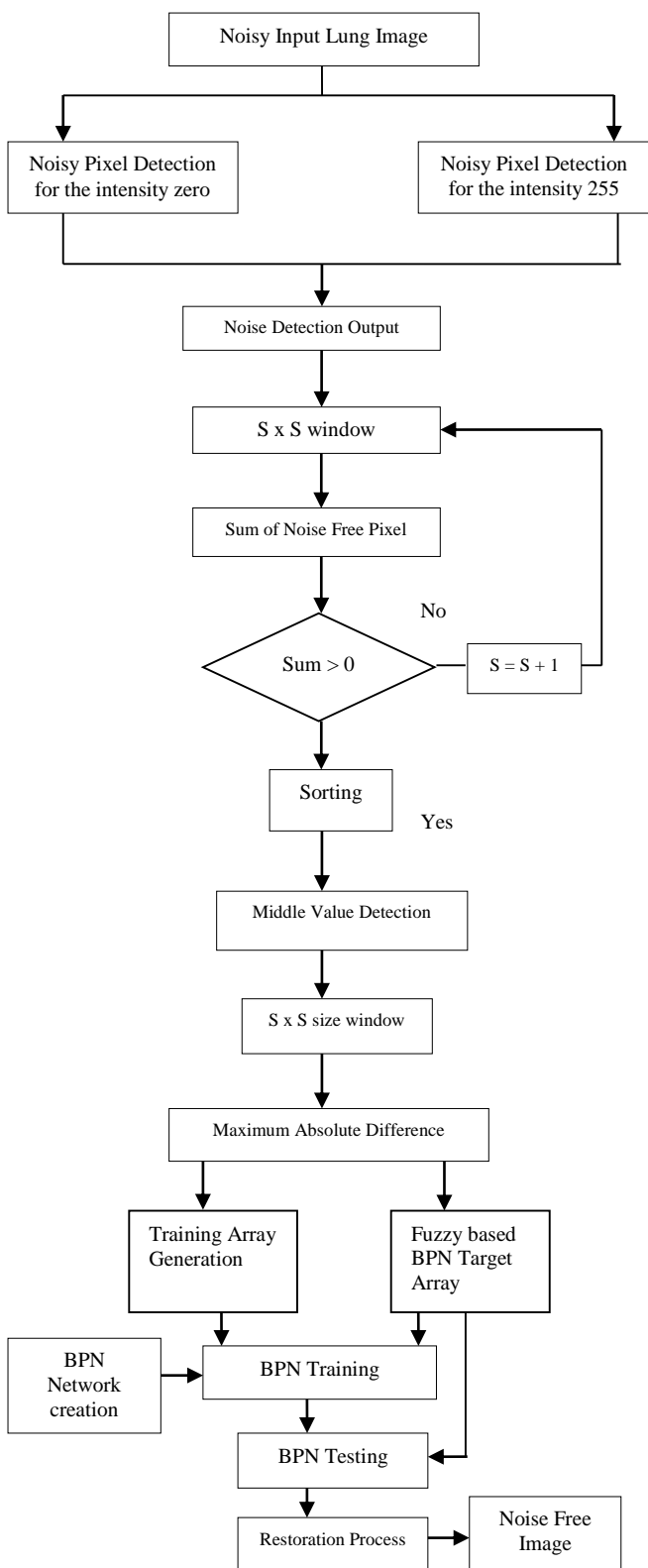
BPN\_net – Trained BPN networks

T – Query noisy 3 x 3 block

NF – Noise Free image

SMF – Switching Median filter Result

Thus the neuro fuzzy based noise reduction is performed.



### SIMULATION RESULTS AND ANALYSIS

The proposed method denoises the impulse noise of medical images. The BPFMSM filter acts on the surface of medical gray scale image in the format like 'bmp'. The databases used in this method are listed below:

- The cancer imaging archive (TCIA) [26]
- The LOLA II [27]

The cancer imaging archive database contains medical brain images which may or may not be affected by cancer tissues. The LolaII database is formed by adding medical lung images in various positions. The analysis part goes ahead with the following two recent noise reduction methods.

- Recursive anisotropic diffusion denoising (RAD) [28]
- Image denoising via Band wise adaptive modeling and regularization exploiting non local similarity (BAM-RNS) [29]

These two papers are implemented and analyzed and the resultant values are tabulated as tables and charts for the performance comparison. The fig.2 explains the outputs of the proposed method for various databases. In the TCIA database 100 images are selected for testing denoising and also 100 images from Lola II database are tested for better comparison work.

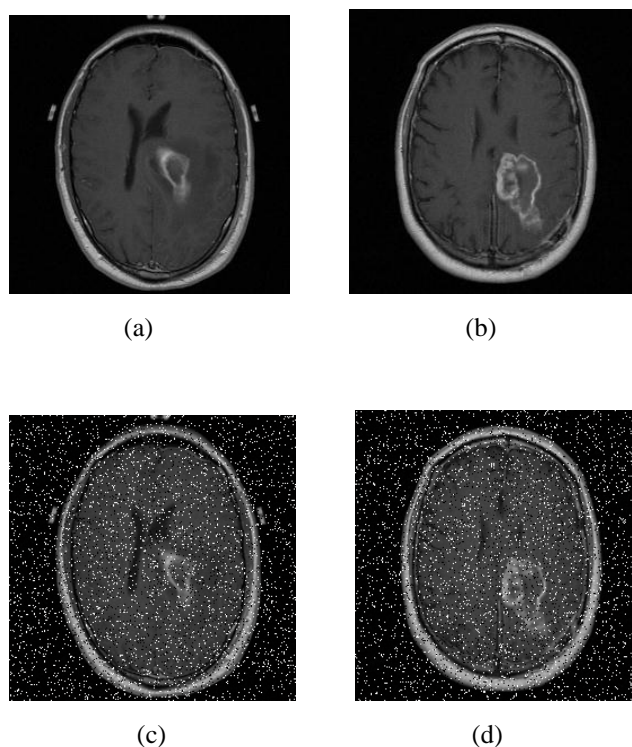
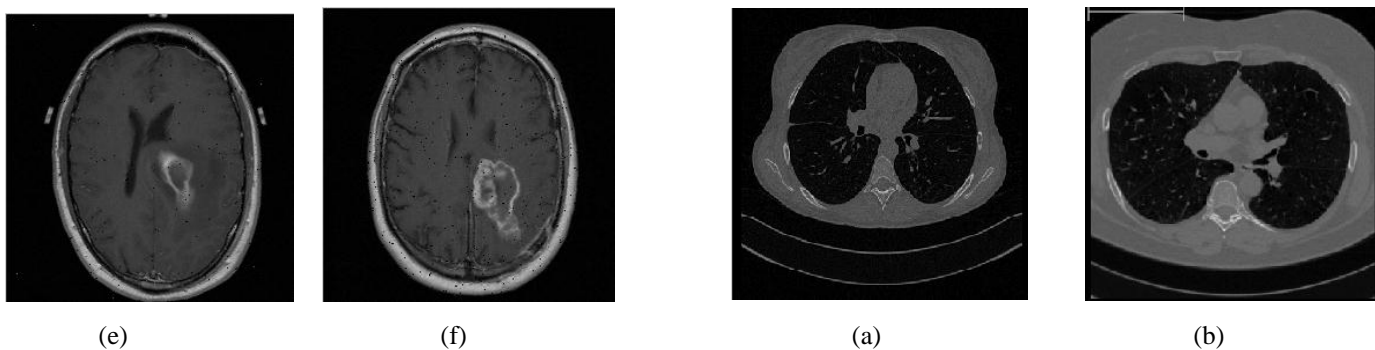
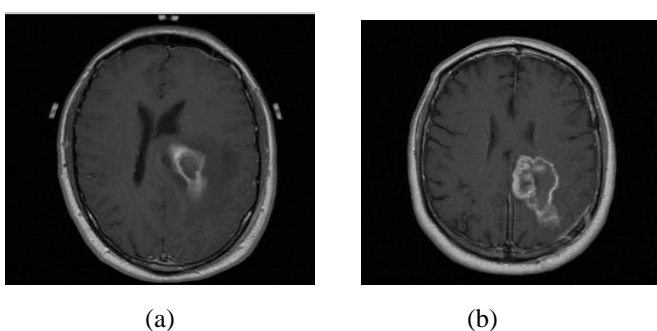


Figure1: Block diagram of proposed BPFMSM noise reduction



**Figure 2:** Noise removal result for 10% noise level on TCIA database Brain images, (a & b) Original images, (c & d) Noise distributed images, (e & f) Denoised outputs.



**Figure 3:** Noise removal result for 50% noise level on TCIA database Brain images, (a&b) Original images, (c&d) Noise distributed images, (e&f) Denoised outputs.

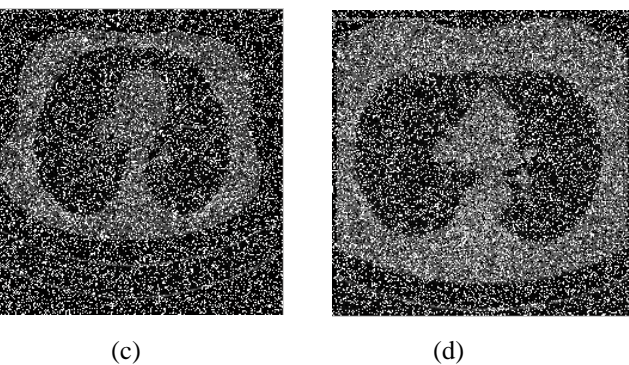
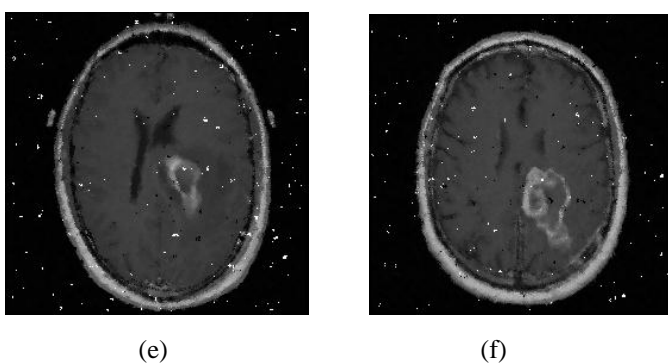


**Figure 4:** Noise removal result for 50% noise level on LOLA11 database lung images, (a&b) Original images, (c&d) Noise distributed images, (e&f) Denoised outputs.

The outputs of the proposed method for 10% and 50% noise corruption level are illustrated in the figures Figure 2, Figure 3 and Figure 4 respectively. The proposed method is working well efficiently for the three types of ratio such as 10% and 50%.



**Table 1:** Peak Signal to Noise Ratio Analysis for 10% noise corruption

| Noise Level | Database Name | Image Name   | Method Name | PSNR |
|-------------|---------------|--------------|-------------|------|
| 10%         | TCIA          | TCIA Brain-1 | RAD[28]     | 36.7 |
|             |               |              | BAM-RNS[29] | 37.2 |
|             |               |              | Proposed    | 40.3 |
|             |               | TCIA Brain-2 | RAD[28]     | 36.1 |
|             |               |              | BAM-RNS[29] | 36.4 |
|             |               |              | Proposed    | 39.7 |
|             | LOLA II       | LOLA Lung-1  | RAD[28]     | 36.4 |
|             |               |              | BAM-RNS[29] | 36.9 |
|             |               |              | Proposed    | 39.4 |
|             |               | LOLA Lung-2  | RAD[28]     | 36.9 |
|             |               |              | BAM-RNS[29] | 37.4 |
|             |               |              | Proposed    | 40.6 |

**Table 2:** Peak Signal to Noise Ratio Analysis for 50% noise corruption

| Noise Level | Database Name | Image Name   | Method Name | PSNR        |      |
|-------------|---------------|--------------|-------------|-------------|------|
| 10%         | TCIA          | TCIA Brain-1 | RAD[28]     | 16.9        |      |
|             |               |              | BAM-RNS[29] | 17.4        |      |
|             |               |              | Proposed    | 19.8        |      |
|             |               | TCIA Brain-2 | RAD[28]     | 16.8        |      |
|             |               |              | BAM-RNS[29] | 17.3        |      |
|             |               |              | Proposed    | 19.2        |      |
|             |               | LOLA II      | LOLA Lung-1 | RAD[28]     | 17.2 |
|             |               |              |             | BAM-RNS[29] | 17.7 |
|             |               |              |             | Proposed    | 19.1 |
|             | LOLA Lung-2   |              | RAD[28]     | 16.9        |      |
|             |               |              | BAM-RNS[29] | 17.2        |      |
|             |               |              | Proposed    | 19.7        |      |

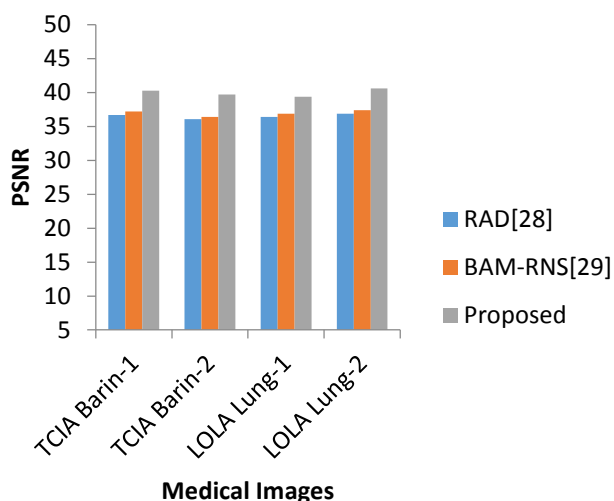


**Figure 5:** PSNR analysis chart for 10% noise level of TCIA and LOLA II databases

The proposed method is well performed in the case of noise reduction at the noise level 10% by obtaining the higher PSNR value as 0.6. The BAM-RNS method is next best method because it owns the PSNR value as 37.4 which come as second position. The higher the PSNR mentions about the best method and lower PSNR indicates lower performance method.

The peak signal to noise ratio is computed using the following equation

$$PSNR = 10 * \log_{10} \left( \frac{255^2}{MSE} \right), \text{ where MSE – Mean Square Error}$$

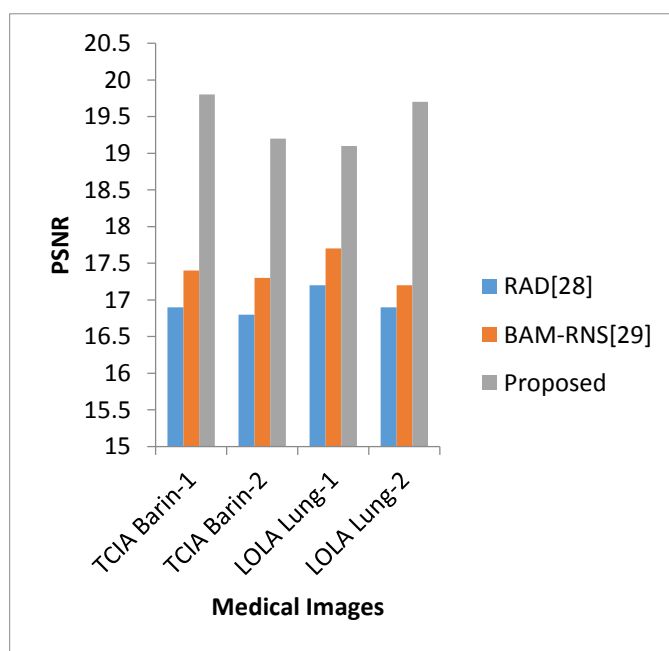


**Figure 6:** PSNR analysis chart for 50% noise reduction

The table 2 and figure 6 also announced the winning of the proposed method BPFMS in the case of noise reduction at 50% noise corruption because of the higher PSNR value as 19.7.

**Table 3:** Eye Perception Index Analysis

|     | Method Name | Eye Perception Index based Rank |
|-----|-------------|---------------------------------|
| 10% | RAD[28]     | 1                               |
|     | BAM-RNS[29] | 2                               |
|     | Proposed    | 3                               |
| 50% | RAD[28]     | 1                               |
|     | BAM-RNS[29] | 2                               |
|     | Proposed    | 3                               |

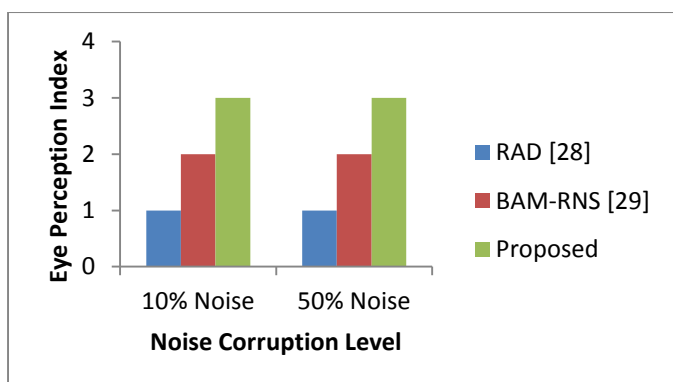


**Figure 7:** Eye perception index based analysis

The eye perception index is computed based on the human perception of eye visual. Table 3 and figure 7 depicts the eye perception index. The outputs of the denoising methods are visually compared and analyzed based on human eye perception and ranked with a condition that better method will own highest rank and lower will own lower rank. According to that criteria the proposed method reaches the higher rank among the existing methods.

**Table 4:** Average Time taken Analysis

|     | Noise Reduction Methods | Time taken (in sec) |
|-----|-------------------------|---------------------|
| 10% | RAD[28]                 | 102                 |
|     | BAM-RNS[29]             | 106                 |
|     | Proposed                | 111                 |
| 50% | RAD[28]                 | 140                 |
|     | BAM-RNS[29]             | 148                 |
|     | Proposed                | 150                 |

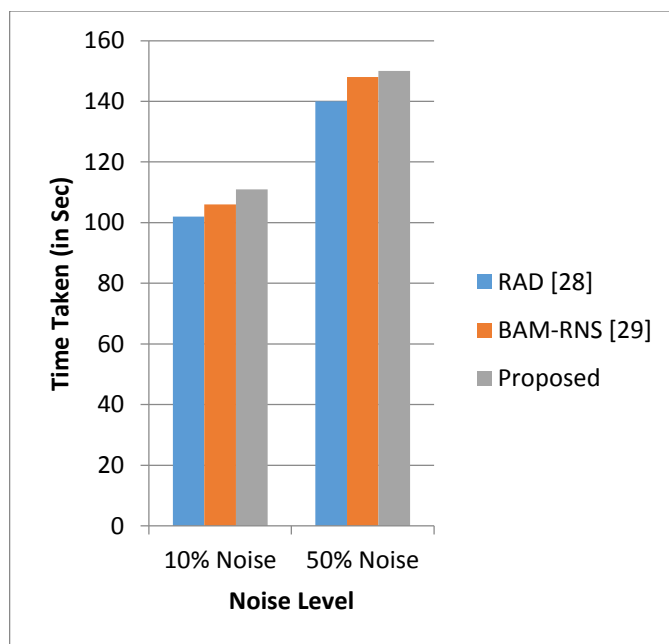


**Figure 8:** Time taken analysis Chart

The table 4 and Figure 8 depicts that the proposed method takes only reasonable run time but when we consider the performance level then this time variation is digestable one.

## CONCLUSION

This research proposes a novel method of denoising scheme in the name BPFMS which removes noises in the type of impulse noise. The proposed method makes the medical lung images as noise free using the powerful combination of neuro fuzzy. The PSNR analysis proves that the proposed BPFMS method is the best denoising method with PSNR 40.6 among the existing denoising researches for 10% noise corruption. The proposed BPFMS method takes only very reasonable time so, this is an agreeable method with better performance. This proposed method is best fit for medical lung image noise reduction because of its unparalleled power of noise reduction. This paper concludes that the proposed BPFMS method is being an algorithm of high rank than existing versions. The hardware implementation of this method can be considered as the future development of this research paper.

## REFERENCES

- [1] M. Bertalmío, *Image Processing for Cinema*. Boca Raton, FL, USA: CRC Press, 2014.
- [2] L. I. Rudin, S. Osher, and E. Fatemi, "Nonlinear total variation based noise removal algorithms," *Phys. D, Nonlinear Phenomena*, vol. 60, nos. 1-4, pp. 259-268, 1992.

- [3] S. P. Awate and R. T. Whitaker, "Higher-order image statistics for unsupervised, information-theoretic, adaptive, image filtering", in *Proc. IEEE Comput. Soc. Conf. Comput. Vis. Pattern Recognition*, vol. 2, Jun. 2005, pp. 44–51.
- [4] A. Buades, B. Coll, and J.-M. Morel, "A non-local algorithm for image denoising", in *Proc. IEEE Comput. Soc. Conf. Comput. Vis. Pattern Recognit.*, vol. 2, Jun. 2005, pp. 60–65.
- [5] H. Tian, B. Fowler, and A. E. Gamal, "Analysis of temporal noise in CMOS photodiode active pixel sensor", *Solid-State Circuits, IEEE Journal of*, vol. 36, no. 1, pp. 92–101, 2001.
- [6] Jayachandiran Jai Jaganath Babu, Gnanou Florence Sudha, "Non-subsampled contourlet transform based imagedenoising in ultrasound thyroid images using adaptive binary morphological operations", *IET Comput. Vis.*, 2014, Vol. 8, Iss. 6, pp. 718–728, doi: 10.1049/iet-cvi.2014.0008
- [7] Donoho, D.L.: "Denoising by soft-thresholding", *IEEE Trans. Inf. Theory*, 1995, 41, pp. 613–627
- [8] Zhi Liu, Shuqiong Xu, C. L. Philip Chen, Yun Zhang, Xin Chen, and Yaonan Wang, "A Three-Domain Fuzzy Support Vector Regression for Image Denoising and Experimental Studies", *IEEE Transactions On Cybernetics*, Vol. 44, No. 4, April 2014.
- [9] H. P. Huang and Y. H. Liu, "Fuzzy support vector machines for pattern recognition and data mining", *Int. J. Fuzzy Syst.*, vol. 4, no. 3, pp. 826–835, 2002.
- [10] C. F. Lin and S. D. Wang, "Fuzzy support vector machines", *IEEE Trans. Neural Netw.*, vol. 13, no. 2, pp. 464–471, Mar. 2002.
- [11] Yehuda Dar, Alfred M. Bruckstein, Michael Elad, and Raja Giryes, "Postprocessing of Compressed Images via Sequential Denoising", *IEEE Transactions on Image Processing*, DOI 10.1109/TIP.2016.2558825
- [12] M. Aharon, M. Elad, and A. Bruckstein, "K-SVD: An algorithm for designing overcomplete dictionaries for sparse representation", *IEEE Trans. Signal Process.*, vol. 54, no. 11, pp. 4311–4322, 2006.
- [13] K. Dabov, A. Foi, V. Katkovnik, and K. Egiazarian, "Image denoising by sparse 3-D transform-domain collaborative filtering", *IEEE Trans. Image Process.*, vol. 16, no. 8, pp. 2080–2095, 2007.
- [14] Khanh Quoc Dinh, Thuong Nguyen Canh, and Byeungwoo Jeon, "Color Image Denoising via Cross-channel Texture Transferring", *IEEE Signal Processing Letters*, DOI 10.1109/LSP.2016.2580711.
- [15] S. Gu, L. Zhang, W. Zuo, and X. Feng "Weighted Nuclear Norm Minimization with Application to Image Denoising", *Proc. IEEE Conf. Computer Vision and Pattern Recognition*, pp. 2862–2869, 2014.
- [16] Alp Ertürk, "Enhanced Unmixing-Based Hyperspectral Image Denoising Using Spatial Preprocessing", *Ieee Journal Of Selected Topics In Applied Earth Observations And Remote Sensing, Digital Object Identifier* 10.1109/JSTARS.2015.2439031.
- [17] A. Ertürk, D. Çeşmeci, M. K. Güllü, D. Gerçek, and S. Ertürk, "Integrating anomaly detection to spatial preprocessing for endmember extraction of hyperspectral images", in *Proc. IEEE Geosci. Remote Sens. Symp. (IGARSS)*, 2013, pp. 1087–1090.
- [18] Gabriela Ghimpețeanu, Thomas Batard, Marcelo Bertalmío, and Stacey Levine, "A Decomposition Framework for Image Denoising Algorithms", *IEEE Transactions On Image Processing*, Vol. 25, No. 1, January 2016.
- [19] Jing Han, Jiang Yue, Yi Zhang, Lianfa Bai, "Local Sparse Structure Denoising for Low-light-level Image", *IEEE Transactions on Image Processing*, DOI 10.1109/TIP.2015.2447735.
- [20] Marc Lebrun, Miguel Colom, Jean-Michel Morel, "The Noise Clinic: a Blind Image Denoising Algorithm", *Image Processing On Line*, vol. 5, pp: 1-54, 2015.
- [21] Fumitaka Hosotani, Yuya Inuzuka, Masaya Hasegawa, Shigeki Hirobayashi, Tadanobu Misawa, "Image denoising with Edge-preserving and segmentation based on Mask NHA", *IEEE Transactions on Image Processing*, DOI 10.1109/TIP.2015.2494461.
- [22] M. Hasegawa, T. Kako, S. Hirobayashi, T. Misawa, T. Yoshizawa, and Y. Inazumi, "Image inpainting on the basis of spectral structure from 2-d nonharmonic analysis", *IEEE Transactions on Image Processing*, vol. 22, no. 8, pp. 3008–3017, 2013.
- [23] Ramy Hussein, Khaled Bashir Shaban, and Ayman H. El-Hag, "Wavelet Transform With Histogram-Based Threshold Estimation for Online Partial Discharge Signal Denoising", *IEEE Transactions On Instrumentation And Measurement*, DOI: 10.1109/TIM.2015.2454651.
- [24] Ido Zachevsky and Yehoshua Y. (Josh) Zeevi, "Statistics of Natural Stochastic Textures and Their Application in Image Denoising", *IEEE Transactions On Image Processing*, Vol. 25, No. 5, May 2016.



- [25] J. Weickert, *Anisotropic Diffusion in Image Processing*. Stuttgart, Germany: Teubner Stuttgart, 1998.
- [26] [www. Cancerimagingarchive.net](http://www.Cancerimagingarchive.net)
- [27] [https:// lola11. grand – challenge. Org / details/](https://lola11.grand-challenge.org/details/)
- [28] V. Ostojic, D. Starcevic and V. Petrovic, “ Recursive anisotropic diffusion denoising”, IET electronics letters, vol.52, issue-17, 2016.
- [29] RuiqunXiong, Hangfan Liu, Xinfeng Zhang, Jian Zhang, Siwei Ma, FengWa and Wen Gao, “ Image denoising via Band wise adaptive modeling and regularization exploiting non local similarity”, IEEE transactions on Image processing, DOI: 10.1109 / TIP.2016.2614160, 2016.